Orientational distribution of spin-labeled actin oriented by flow

E. Michael Ostap, Toshio Yanagida,* and David D. Thomas
Department of Biochemistry, University of Minnesota Medical School, Minneapolis, Minnesota 55455 USA; and
*Department of Biophysical Engineering, Osaka University, Toyonaka, Osaka, Japan

ABSTRACT Previous studies on spin-labeled F-actin (MSL-actin), using saturation transfer electron paramagnetic resonance (ST-EPR), have demonstrated that actin has submillisecond rotational flexibility and that this flexibility is affected by the binding of myosin and its subfragments. This rotational flexibility does not change during the active interaction of myosin heads, actin, and adenosine triphosphate. However, these ST-EPR studies, performed on randomly oriented actin, would not be sensitive to orientational changes on the millisecond time scale or slower. In the present study, we have clarified these results by performing conventional EPR experiments on MSL-actin oriented by flow to detect changes in the orientational distribution. We have determined the orientational distribution of the spin labels relative to the magnetic field (flow direction) by comparing experimental EPR spectra to simulated EPR spectra corresponding to known orientational distributions. Spectra acquired during flow indicate two populations of probes: a highly ordered population and a disordered population. For the ordered population (28% of the total spin concentration), the angle between the actin filament axis and the nitroxide z axis (θ) fits a Gaussian distribution centered at 32.0 ± 0.9°, with a full width at half maximum of 20.7 ± 3.9°. The angle between the nitroxide x axis and the projection of the field in the xy plane (ϕ) is centered at 37.5 ± 9.2° with a full width of 24.9 ± 10.7°. This orientational distribution is not significantly changed upon the binding of phalloidin or myosin subfragment 1 (S1), indicating that these proteins do not affect the axial orientation of actin subunits. Spectra of spin-labeled S1 (MSL-S1) bound to actin oriented by flow have about the same orientational distribution as MSL-S1 bound to actin in oriented fibers. Thus, the oriented fraction of flow-oriented actin filaments has nearly the same high degree of alignment as the actin filaments in muscle fibers.

INTRODUCTION

Force generation during muscle contraction arises from the direct interaction of myosin and actin, coupled to a cycle of adenosine triphosphate (ATP) hydrolysis. According to the rotating cross-bridge model, the pivoting motion of a myosin head attached to actin produces strain, which is then relieved by the sliding motion of the myosin and actin filaments (Reedy et al., 1965; Huxley, 1969; Huxley and Simmons, 1971). This myosin rotation is generally modeled as movement of the myosin head relative to the actin filament. Alternatively, it has also been proposed that the ATP-induced myosin head rotation may originate with motions of the actin itself (Huxley, 1974). To obtain a complete description of the physical basis of this dynamic energy transduction, direct measurements of the molecular dynamics of myosin and actin are required.

Conventional electron paramagnetic resonance spectroscopy (EPR), to measure orientation, and saturation transfer electron paramagnetic resonance spectroscopy (ST-EPR), to measure microsecond rotational motion, have proven to be particularly useful in the studies of the molecular dynamics of both myosin and actin in solution and in fibers. EPR allows for the detection of site-specific probes (spin labels) that provide the kind of selectivity not possible with mechanical or x-ray diffraction studies (for a review, see Thomas, 1987).

Because most models of muscle contraction consider the myosin head as the active component in force generation, EPR studies have targeted the rotational motions and orientational distributions of the myosin head (e.g., Thomas and Cooke, 1980; Cooke et al., 1982; Barnett et al., 1986; Berger et al., 1989; Barnett and Thomas, 1989; Fajer et al., 1991). However, a number of investigations suggest that actin undergoes conformational changes upon the binding of S1 and that these changes are necessary for the activation of muscle contraction (e.g., Prochniewicz-Nakayama and Yanagida, 1982; Miki et al., 1987; Prochniewicz and Yanagida, 1990). Previous studies on spin-labeled F-actin, using ST-EPR, have demonstrated that actin has submillisecond rotational flexibility and that this flexibility is affected by the binding of myosin and its subfragments (Thomas et al., 1979; Mossakowska et al., 1988; Ostap and Thomas, 1991). However, it also has been shown that the active interaction of S1, actin, and ATP does not affect the microsecond rotational motion of spin-labeled actin, despite the greatly increased motion of actin-bound myosin heads (Berger et al., 1989; Ostap and Thomas, 1991).

The geometric details of these rotational motions are unknown because the orientational distributions of the spin labels with respect to the filament axis are unknown. Also, EPR investigations that would detect orientational changes of actin filaments upon the binding of myosin heads have not been pursued rigorously. To detect orientational changes in the actin filament with EPR, it would be best to spin-label actin specifically in muscle fibers. However, specific labeling of cys-374 of actin in muscle fibers has not been achieved. This is due to the large number of proteins, other than actin, that readily react with sulfhydryl-directed spin labels in the muscle fiber. Therefore, an approach must be taken to orient solutions of purified actin for study in EPR experiments. Previously, investigators have oriented actin in strong magnetic fields (Torbet and Dickens, 1984), by

Address correspondence to Dr. D. D. Thomas.

0006-3495/92/10/966/10 $2.00

the flow of actin solutions (Miki and Mihashi, 1977), by the flow of actin sols (Popp et al., 1987), and by the electrophoresis of actin in agarose gels (Borejdo and Ortega, 1989). In the present study, we have oriented actin solutions by flow and determined the orientational distribution of the spin labels rigidly bound to actin. The orientational distributions were determined in the presence and absence of S1 by comparing experimental EPR spectra to simulated EPR spectra corresponding to known orientational distributions, using the Amoeba method (Fajer et al., 1990*a*).

METHODS

Solutions and protein preparations

F-actin was prepared by the method of Pardee and Spudich (1982). Chymotryptic S1 was prepared as described by Eads et al. (1984), except that the chymotryptic digestion time was 10 min. Glycerinated psoas muscle fibers from New Zealand white rabbits were prepared by chemical skinning in 0.5% Triton X-100 and glycerination in 25% glycerol as described in Fajer et al. (1988). F-actin was spin-labeled at cys-374 with 4-maleimido-2,2,6,6,-tetramethyl-1-piperidinyloxy (MSL; Aldrich Chemical Co., Milwaukee, WI) to the extent of 0.96 ± 0.03 label bound per actin monomer (Ostap and Thomas, 1991). S1 was spin-labeled with MSL to the extent of 0.98 ± 0.02 label bound per head, with 100 ± 0.04% of these labels specifically bound to cys 707 or cys 697, as previously described (Svensson and Thomas, 1986). Protein concentrations were determined spectrophotometrically with the following extinction coefficients: 0.63 mg^{-1} ml cm^{-1} at 290 nm for G-actin (Houk and Ue, 1974) and 0.74 mg^{-1} ml cm^{-1} at 280 nm for S1 (Margossian and Lowey, 1982). The molecular weight was assumed to be 42,500 for actin and 109,000 for S1. Polymerized actin and S1 were dialyzed into solutions containing 130 mM potassium propionate, 25 mM MOPS, 1 mM $MgCl_2$, 1 mM NaN_3, pH 7.0 (25°C). In the experiments that required ATP, 5 mM ATP was added to the actin solution immediately before the experiment. In the experiments that required phalloidin, a saturating amount of phalloidin (Calbiochem, San Diego, CA) was added to the F-actin solution.

Electron paramagnetic resonance

EPR experiments were performed on an ESP 300 spectrometer (Bruker Instruments, Inc., Billerica, MA). EPR spectra of randomly oriented MSL-actin were acquired using a TE_{102} EPR cavity (ER4102 ST; Bruker Instruments), with samples contained in a 20 μl well on a TPX cover plate that was attached to a quartz flat cell (WG-807; Wilmad Glass Co. Inc., Buena, NJ). The MSL-actin was placed on the cover plate and mixed. The cover plate was then attached to the flat cell, avoiding any flow of the actin solution. Flow experiments (oriented actin and oriented fiber bundles) were performed using a TM_{110} cavity (ER4103 TM; Bruker Instruments) modified to accept a capillary tube parallel or perpendicular to the static magnetic field. EPR spectra were obtained using a peak-to-peak modulation amplitude of 2 G with a microwave field intensity of 0.032 G as calculated from cavity Q and peroxylamine disulfonate (PADS) calibrations (Squier and Thomas, 1986). EPR spectra were acquired and digitized with the spectrometer's built-in microcomputer, using ESP 1620 spectral acquisition software (Bruker Instruments) and were then transferred to an IBM-compatible microcomputer. The temperature of the sample was maintained by using a variable temperature controller (ER4111; Bruker Instruments). All spectra were acquired at 25 ± 1.0°C unless stated otherwise. Within each figure, experimental spectra have been normalized to correspond to the same number of spins by dividing by the double integral of the EPR spectrum. Each simulated component spectrum is plotted to represent the corresponding mole fraction.

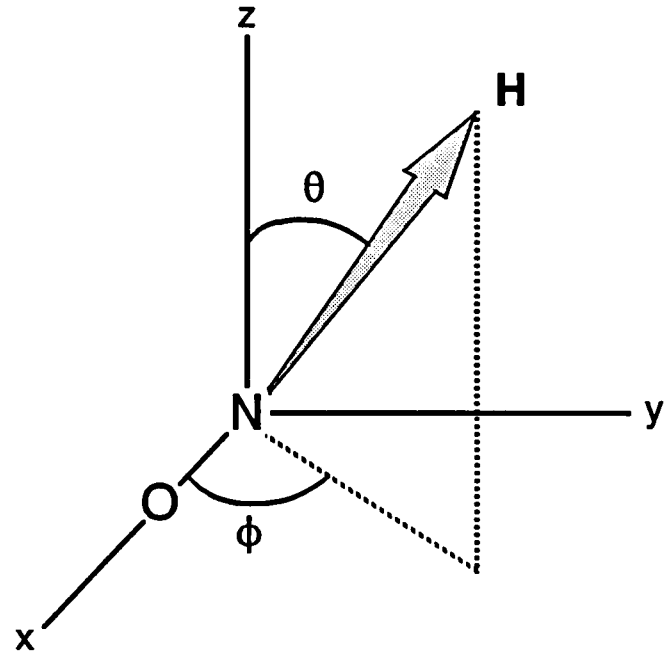

FIGURE 1 Definitions of the angles θ and ϕ, which define the orientation of the magnetic field H with respect to the principal axes of a nitroxide spin label. These angles determine the orientational dependence of the EPR spectrum.

F-actin was oriented by flowing a 100 μM solution at a rate of 500 μl/min through a capillary tube with an inner diameter of 0.75 mm. Flow was maintained by a peristaltic pump (Microperpex, LKB 2132; LKB Instruments Inc., Bromma, Sweden). Actin-S1 solutions were oriented as described in Results. Muscle fiber bundles (0.5 mM) were placed in 1-mm glass capillaries and held isometrically by surgical thread tied to the bundle ends. Solutions were continuously flowed over the fibers at a rate of 200 μl/min.

Spectral analysis and computer fitting

The magnetic field axis (center field and scan width) of each spectrum was calibrated with a spectrum of 0.9 mM PADS in 50 mM K_2CO_3 recorded on the same day and in the same sample configuration as the experimental spectra. The PADS splitting was assumed to be 13.091 G (Faber and Fraenkel, 1967). All spectra, experimental and simulated, were aligned or calculated so that the center corresponded to a g value of 2.0056, which is the center of the PADS spectrum (Fajer et al., 1990*b*). This alignment allowed the experimental spectra to be compared directly with other experimental and simulated spectra.

The experimental spectra were condensed to 512 points and were fitted by using the Amoeba method, a χ^2 minimization routine, using a Cray 2 Supercomputer (Minnesota Supercomputer Institute) (Fajer et al., 1990*a*, *b*). Angle-independent parameters were obtained by fitting EPR spectra of unoriented MSL-actin by simultaneous optimization of 11 tensor and line-width parameters. Because it has been shown that there is no nanosecond rotational motion of MSL relative to actin, the EPR spectrum is determined by the orientational distribution $\rho(\theta, \phi)$, where θ and ϕ are the axial (tilt) and azimuthal (twist) angles of the magnetic field H (which defines the direction of the average actin filament axis) relative to the nitroxide-fixed axes x, y, and z (Fig. 1). The spin labels were assumed to have a Gaussian distribution of full width $\Delta\theta$ about the average tilt angle θ_0, with a probability distribution $\rho(\theta) = \exp[-(\ln 2)\{(\theta - \theta_0)/\Delta\theta/2\}^2]$. A similarly defined distribution $\rho(\phi)$ was assumed for the twist angle ϕ (Fig. 1). The disorder about the twist angle ($\Delta\phi$) is not the azimuthal disorder of the actin monomers in the

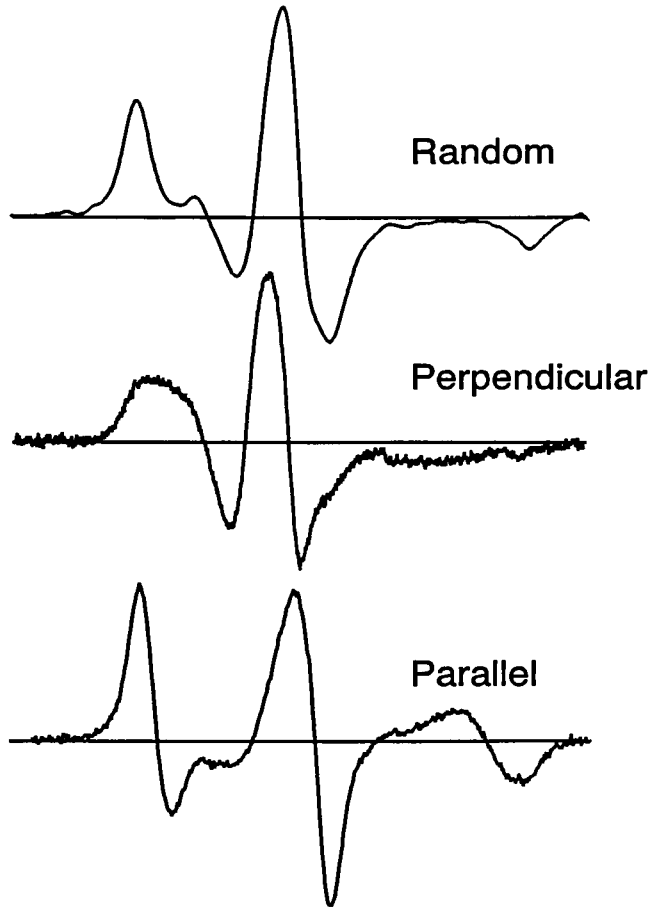

FIGURE 2 Conventional EPR spectra of 100 μM MSL-actin (*top*) randomly oriented, (*center*) flowing perpendicular to the magnetic field, and (*bottom*) flowing parallel to the magnetic field.

filament as described by Egelman et al. (1982). The EPR spectrum is sensitive only to the axial orientational distribution of F-actin, which can affect $\rho(\theta)$ and/or $\rho(\phi)$, depending on the orientation of the spin label relative to actin. The total probability distribution is $\rho(\theta, \phi) = \rho(\theta)\rho(\phi)$, which is characterized by the four input parameters θ_0, ϕ_0, $\Delta\theta$, and $\Delta\phi$. The details of the simulations and of the fitting procedures have been described by Fajer et al. (1990*a*).

RESULTS

Conventional EPR of MSL-actin

The reaction of MSL with F-actin has been shown to be very specific for cys-374 under the described labeling conditions (Thomas et al., 1979). Double integration of EPR spectra showed that MSL-actin contained 0.96 ± 0.03 spin labels per actin monomer, so virtually every actin monomer in the MSL-actin preparation is specifically labeled (Ostap and Thomas, 1991). Therefore, any measured properties (e.g., S1 binding) are representative of the spin-labeled actin, as characterized previously. Denatured or incompletely polymerized actin exhibits a weakly immobilized component in the conventional EPR spectrum (Thomas et al., 1979). This component represents <2% of the spin label in the observed spectra (Fig. 2, *top*). This result not only implies that the spin-labeled actin is virtually all in its native polymerized state but also ensures that the spectra of oriented MSL-actin filaments are reliable indicators of the spin label's orientational distribution.

Fig. 2 shows the conventional EPR spectra of MSL-actin (Fig. 2, *top*) randomly oriented in a flat cell in the absence of flow (Fig. 2, *center*), in a solution flowing through a capillary tube oriented perpendicular to the magnetic field, and (Fig. 2, *bottom*) in a solution flowing through the capillary tube parallel to the magnetic field. The large difference in line-shape between the spectra of the samples flowing perpendicular and parallel to the magnetic field (Fig. 2, *center* and *bottom*) indicates that (*a*) the actin filaments are oriented by flow in the capillaries and (*b*) the actin-bound spin labels assume a preferred orientational distribution relative to the actin filament axis (Thomas and Cooke, 1980). The significant features of the spectrum of MSL-actin flowing parallel to the magnetic field (Fig. 2, *bottom*) are the intense and narrow low-field peak and the positive high-field peak. These features are indicative of high orientation (Barnett et al., 1986). If the MSL-actin were not oriented, or if there were no preferred angular distribution of spin labels on the oriented actin, the spectra of the samples flowing parallel and perpendicular to the magnetic field would both resemble Fig. 2 (*top*).

The spectrum of MSL-actin in the flat cell was unchanged by rotation of the cell relative to the magnetic field, indicating random orientation. The spectra of the flowing actin (Fig. 2, *center* and *bottom*) were unchanged by either an increase in flow rate or a decrease in capillary diameter, indicating that further orientation by flow is unlikely.

Determination of angle-independent spectral parameters

The accurate determination of the magnetic tensor values and line-width parameters is a prerequisite for high-resolution determination of the angular distribution from spectra of oriented samples (Fajer et al., 1990*a, b*). These parameters are most accurately determined by analyzing the spectrum of a randomly oriented sample, for which the spectrum is determined entirely by these parameters (Fajer et al., 1990*a, b*). Spectra of randomly oriented actin filaments were acquired and computer fitted (see Methods). The fit resulted in an accurate reproduction of the experimental spectrum (Fig. 3). The values of the tensors and line-width parameters are given in Table 1. The deviation between the experimental spectrum and the simulated spectrum, obtained from the tensors and line-width parameters, may be partially due to small amounts (<2%) of denatured or incompletely polymerized actin, which exhibits a minor component in the EPR spectrum characteristic of weakly immobilized spin labels (Thomas et al., 1979; Ostap and

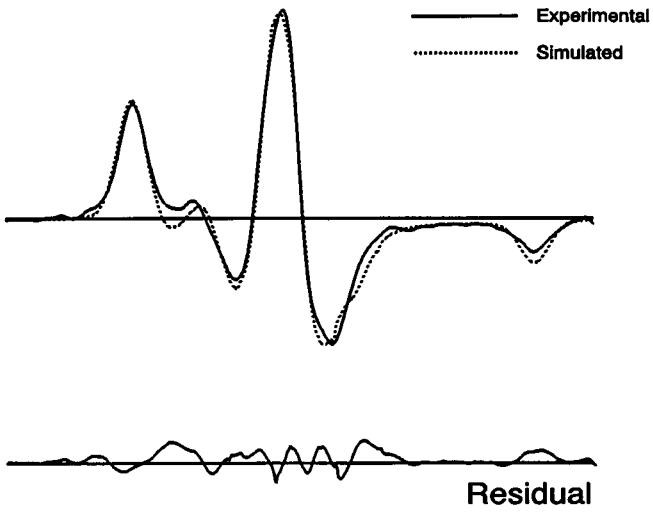

FIGURE 3 Spectral fit of randomly oriented MSL-actin (Fig. 2, *top*) to determine the orientation-independent tensor and line-width parameters in Table 1. (*Solid line*) Experimental spectrum; (*dotted line*) computer fit. The residual (experiment minus the fit) is shown below.

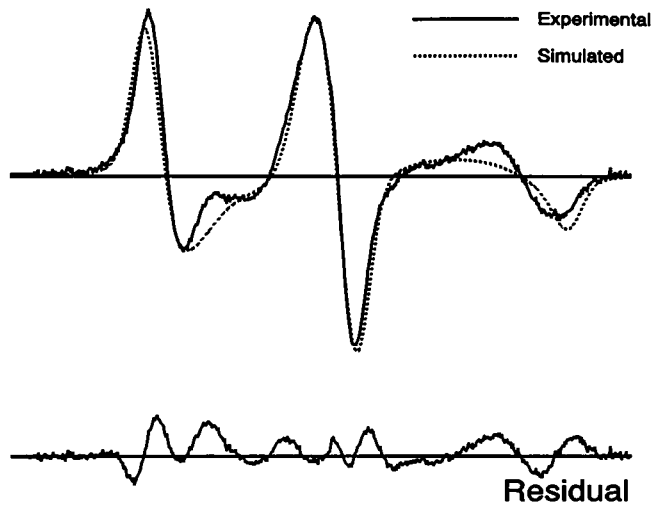

FIGURE 4 Single-component fit to a spectrum of 100 μM MSL-actin flowing parallel to the magnetic field to determine the orientational distribution (Table 2, *first row*). (*Solid line*) Experimental spectrum; (*dotted line*) computer fit. The residual (experiment minus the fit) is shown below.

Thomas, 1991). The deviations also may be due to small errors in the line-width functions (Fajer et al., 1990*a*). These two errors are the most apparent in the residual.

Orientational distribution of MSL-actin oriented by flow

The spectrum of 100 μM MSL-actin flowing parallel to the magnetic field (Fig. 2, *bottom*) was first fitted by assuming a single orientational population with Gaussian distributions of the two angles (full width $\Delta\theta$, $\Delta\phi$), about average values (θ_0, ϕ_0) (Fajer et al., 1990*b*). The values of the four parameters were not constrained; each was allowed to vary between 0 and 90°. The resulting computer fit (Fig. 4, Table 2) was good, but the residual spectrum showed significant disagreement, especially in the high-field part of the experimental spectrum. The sharper high-field peaks of the experimental spectrum clearly indicate a narrower Gaussian distribution ($\Delta\theta$) about the average angle θ_0 than found by the computer fit (Barnett et al., 1986).

To obtain a more accurate fit to the MSL-actin spectrum, a linear combination of two Gaussian orientational distributions (a linear combination of two single-distribution spectra) was assumed. The two spectral components were assumed to have the same magnetic tensors and line-widths but different angular distributions (Fajer et al., 1990*b*). In the fitting of the two components, the values of θ_0 and $\Delta\theta$ of the first component (component A) were restricted between the angles 0 and 45°. This restriction was justified by the measurement of the spectral splitting (2T′) and the splitting of the high-field peaks (ΔH^{pp}) (Barnett et al., 1986; Fajer et al., 1990*a*). All other angles were allowed to vary between 0 and 90°. The resulting two-component fit is a significant improvement over the single-component fit (Fig. 5, Table 2). The χ^2 value improved 5–10-fold over the single-component fit, and the residual is much smaller (Fig. 5, *top left*). The two distributions that were identified are a highly ordered population (component A) and a disordered population (component B). Component A represents ~28% of the total spin-label concentration, and component B makes up the remaining 72% (Table 2). The spectra and orientational distributions of these two populations are shown in Fig. 5, *bottom*. The individual components are normalized to illustrate their respective

TABLE 1 **Magnetic tensors and line-width parameters***

Parameter	Found
g_x	2.00859 ± 0.00007
g_y	2.00535 ± 0.00004
g_z	2.00220 ± 0.00007
T_x	8.76 ± 0.12
T_y	7.71 ± 0.22
T_z	34.30 ± 0.10
Γ_L	0.01 ± 0.02
$\Gamma_{L\theta}$	0.90 ± 0.13
$\Gamma_{L\phi}$	0.29 ± 0.05
Γ_G	2.59 ± 0.19
Γ_{mG}	0.13 ± 0.13

* g denotes the g tensor (unitless) and T the hyperfine tensor (in Gauss). Γ_L and Γ_G are orientationally independent Lorentzian and Gaussian linewidths (in Gauss). $\Gamma_{L\theta}$ and $\Gamma_{L\phi}$ are the θ- and ϕ-dependent Lorentzians, and Γ_{mG} is the manifold-dependent Gaussian. All of these parameters, the equations in which they are used, and the computational procedures used to simulate and fit EPR spectra, have been discussed in detail by Fajer et al. (1990*a*, *b*). Line-widths are reported as half-width at half maximum. Errors are the standard deviations of six searches.

TABLE 2 **Gaussian orientational distributions***

Sample‡	Component A§				Component B				
	θ_0	$\Delta\theta$	ϕ_0	$\Delta\phi$	θ_0	$\Delta\theta$	ϕ_0	$\Delta\phi$	X_A
MSL-actin (2, 10)	31.7 ± 2.0	52.8 ± 4.8	43.6 ± 3.3	50.4 ± 35.5	—	—	—	—	—
MSL-actin (3, 12)	32.0 ± 0.9	20.7 ± 3.9	37.5 ± 9.2	24.9 ± 10.7	45.2 ± 8.5	53.7 ± 9.6	44.5 ± 1.6	80.7 ± 13.6	0.28 ± 0.4
MSL-actin + S1 (1, 7)	32.0 ± 0.3	19.8 ± 0.6	36.1 ± 1.1	41.3 ± 17.8	39.5 ± 0.3	53.9 ± 0.2	45.5 ± 0.1	90.0 ± 0.1	0.20 ± 0.01
Fiber + MSL-S1 (1, 4)	80.8 ± 0.0	18.8 ± 0.0	26.1 ± 0.0	31.3 ± 0.0	—	—	—	—	—
Actin + MSL-S1 (1, 4)	79.5 ± 0.1	15.9 ± 0.6	27.6 ± 0.3	20.6 ± 5.0	50.9 ± 0.4	51.6 ± 0.2	51.4 ± 0.2	4.54 ± 4.11	0.31 ± 0.02

* All values are in degrees.
‡ The first number in parentheses is the number of different protein preparations and the second is the number of computer searches.
§ The errors are the standard deviations resulting from the searches and should be taken as the lower bound for the error (see Discussion).

mole fractions. The convolutions of these components are also shown (Fig. 5, *top*).

The mole fraction of component A did not change significantly (<5%) as a function of the actin preparation, actin concentration (50–200 μM), flow rate (250–1,000 μl/min), capillary size (0.5–1.0 mm), or temperature (4–25°C). The mole fraction and orientational distribution of component A also did not change on the addition of 100 μM phalloidin.

Orientational distribution of oriented actin + S1

The spectrum of 100 μM MSL-actin plus 100 μm S1 flowing parallel to the magnetic field resembles an unori-

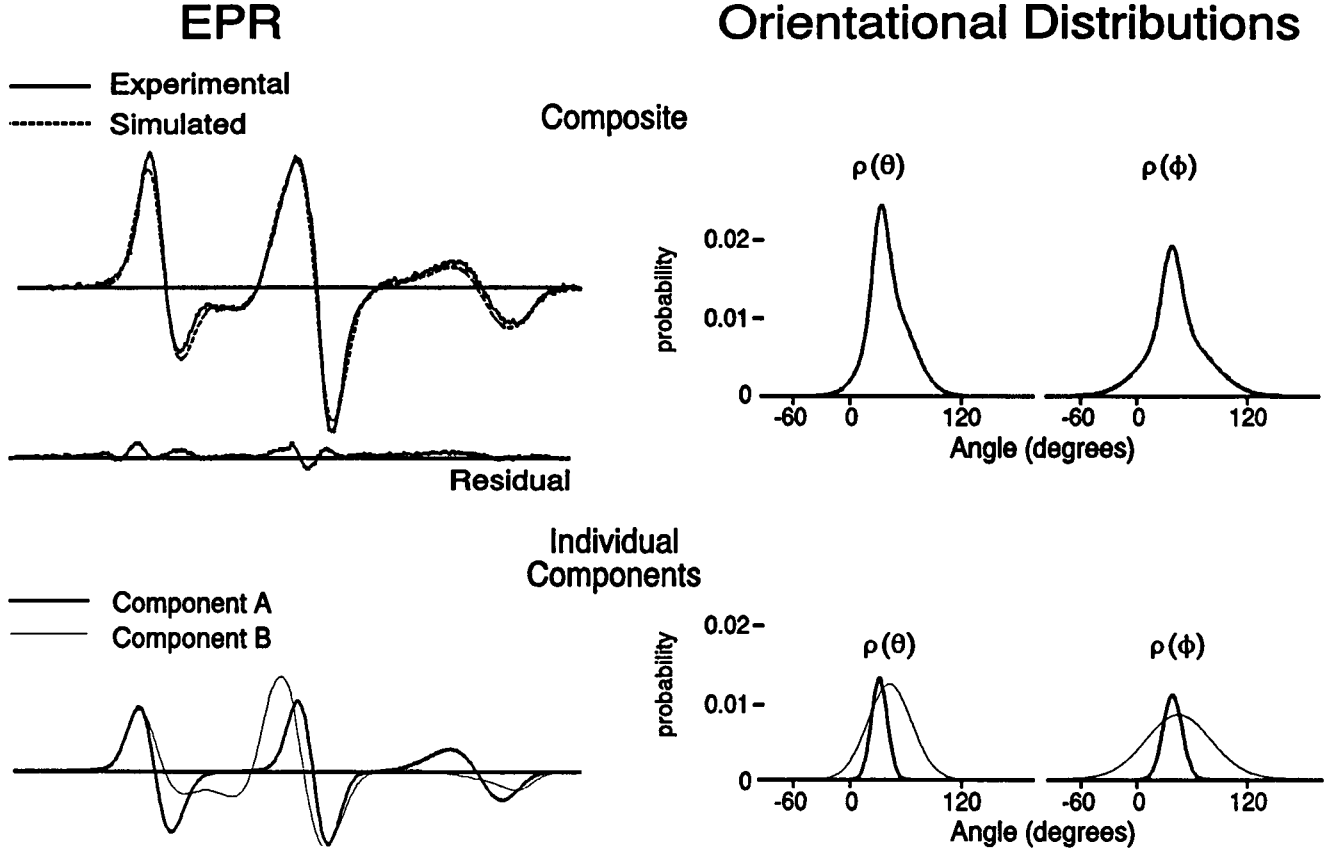

FIGURE 5 Two-component fit to a spectrum of 100 μM MSL-actin flowing parallel to the magnetic field to determine the orientational distributions (Table 2, *second row*). (*left, top*) Overlay of the best-fit simulated spectrum (*dotted line*) and the experimental spectrum (*solid line*). The residual (experiment minus the fit) is shown below. (*left, bottom*) The two simulated components obtained from the computer fit normalized to their respective mole fractions, component A (*thick line*) and component B (*thin line*). (*right, top*) Composite distributions of $\rho(\theta)$ and $\rho(\phi)$. (*right, bottom*) Individual components of the orientational distributions normalized to their respective mole fractions, component A (*thick line*) and component B (*thin line*).

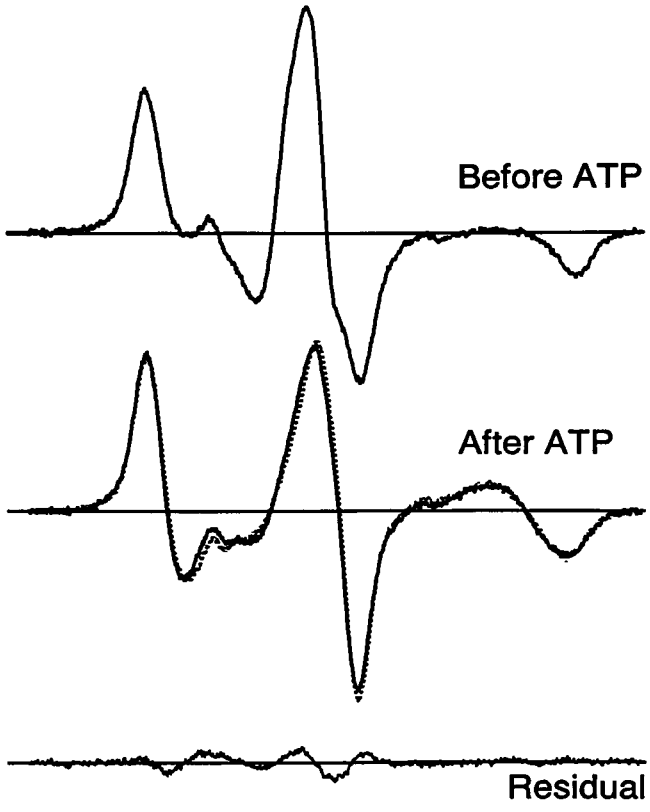

FIGURE 6 The effect of S1 on conventional EPR spectra of MSL-actin solutions parallel to the magnetic field. (*top*) 100 μM MSL-actin in the presence of S1 before the addition of 5 mM MgATP; (*center, solid line*) 100 μM MSL-actin in the absence of S1; (*center, dotted line*) 100 μM MSL-actin in the presence of S1 after the addition and depletion of 5 mM Mg ATP. (*bottom*) The spectrum of MSL-actin minus spectrum of MSL-actin in the presence of S1. Parameters of the orientational distributions are in Table 2, third row.

ented powder spectrum (Fig. 6, *top*). This disorder was observed at S1/actin ratios down to 0.1. It has been demonstrated previously that S1 causes interfilament cross-links between actin filaments, forming actin aggregates (Ando and Scales, 1985; Ando, 1987; Ostap and Thomas, 1991). Presumably, the lack of orientation in the MSL-actin + S1 spectrum is due this S1-induced aggregation, preventing the orientation of the actin filaments.

To orient the MSL-actin + S1, 5 mM MgATP was added to the protein solution, dissociating the S1 from the actin filaments. The MgATP-containing protein solution was rapidly flowed into the capillary tube, orienting the actin filaments. Once the solution had entered the capillary tube, the flow was stopped. As the MgATP was depleted, the S1 reattached to the oriented actin filaments. The resulting EPR spectrum (Fig. 6, *center, dotted line*) is very similar to that of oriented actin (Fig. 2, *center, solid line*), indicating a significant degree of orientation. Computer fits indicate that the orientational distribution of the oriented MSL-actin + S1 was similar to that of MSL-actin in the absence of S1 (Fig. 6, Table 2). For the highly oriented component A, all four angular parameters were within experimental errors for the two samples. However, the mole fraction of component A was smaller than the value obtained in the absence of S1, probably indicating S1-induced disorder (aggregation). The small residual, obtained by the subtraction of the MSL-actin spectrum minus the MSL-actin + S1 spectrum, in Fig. 6 (*bottom*) is due to a difference in the mole fractions of the components. Resuming the flow of the protein solution resulted in a large increase in disorder (data not shown). The data in Fig. 6 and Table 2 constitute direct evidence that no significant axial orientational changes in MSL-actin occur on the binding of S1.

To compare the orientation of the actin filaments oriented by flow with the orientation of actin in the thin filaments of glycerinated muscle fibers, spectra of spin-labeled S1 (MSL-S1) decorated muscle fibers were compared with spectra of MSL-S1 bound to actin oriented by flow. The spectrum of MSL-S1 bound to unoriented actin filaments resembles the spectrum of MSL-S1 in solution, indicating complete orientational disorder (data not shown). Spectra of MSL-S1 decorated fibers and spectra of oriented solutions of 100 μM actin and 100 μM MSL-S1 were acquired and computer fitted (Table 2). The tensor and line-width parameters used in the fits were determined previously (Barnett et al., 1986; Fajer et al., 1990*b*). The spectrum of the MSL-S1 bound to the oriented actin was fitted assuming two orientational distributions, and the spectrum of MSL-S1 bound to actin in the oriented fibers was fitted assuming a single orientational distribution. The fit of the MSL-S1 decorated fibers resulted in an orientational distribution very similar to that previously reported (Barnett et al., 1986; Fajer et al., 1990*b*). As expected, the fit of the spectrum of MSL-S1 bound to actin oriented by flow resulted in a highly ordered component and a disordered component resembling a powder spectrum. Fig. 7 shows (*left*) the spectrum of MSL-S1 decorated fibers and (*right*) the spectrum of MSL-S1 bound to actin oriented by flow. The individual components normalized to their respective mole fractions are shown below the spectra. The spectra, and thus the orientational distributions (Table 2), of the ordered components are very similar. Thus, the oriented fraction of flow-oriented actin filaments has nearly the same high degree of alignment as the actin filaments in muscle fibers.

DISCUSSION

Summary and interpretation of results

The purpose of this investigation was to determine the orientational distributions of spin labels bound to oriented actin and to determine whether these orientational

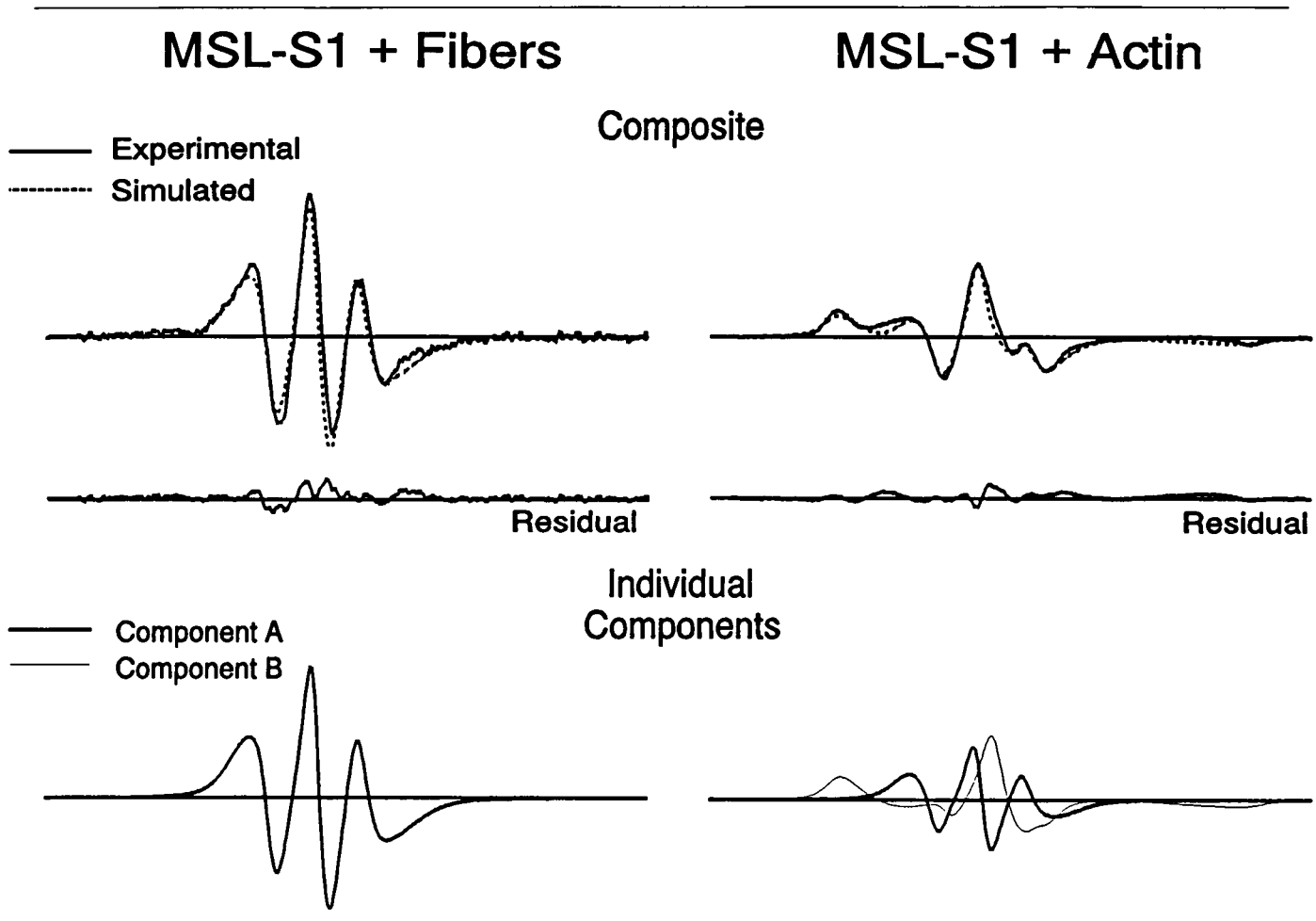

FIGURE 7 Experimental and best-fit simulated EPR spectra of MSL-S1 bound to actin in muscle fibers and in solution. (*left, top*) Overlay of the spectrum of MSL-S1 bound to actin in glycerinated muscle fibers oriented parallel to the magnetic field (*solid line*) and the best-fit simulated spectrum (*dotted line*). The residual (experiment minus the fit) is shown below. (*left, bottom*) The simulated spectrum normalized to its double integral. (*right, top*) Overlay of the spectrum of MSL-S1 bound to actin oriented by flow (*solid line*) and the best-fit simulated spectrum (*dotted line*). The residual is shown below. (*right, bottom*) Individual components of the orientational distributions normalized to their respective mole fractions, component A (*thick line*) and component B (*thin line*). The parameters defining the orientational distributions are in Table 2, fourth and fifth rows.

distributions change upon the binding of S1. The orientational resolution of the nitroxide EPR spectrum makes spin labels uniquely powerful in the study of molecular orientation in organized systems. When a spin-labeled sample is macroscopically ordered (e.g., actin in a muscle fiber), the EPR spectrum allows different orientations to be directly resolved, so populations of probes that differ in orientation by a few degrees can be detected independently (Thomas, 1987). However, a principal difficulty is in selectively spin-labeling a single class of sites in the muscle fiber (Thomas and Cooke, 1980). The attachment of spin labels exclusively to cys-374 of actin in muscle fibers has not been achieved. Therefore, we have created an organized system of oriented actin filaments by flowing actin solutions through a capillary tube oriented parallel to the static magnetic field.

For a spin label to report reliably the molecular orientation of a protein, (*a*) it must be rigidly bound to the protein (i.e., it must not have nanosecond rotational mobility relative to the protein) and (*b*) it must be stereospecifically bound to a single site on the protein. MSL-actin satisfies both of these requirements. It has been reported previously that MSL is rigidly bound to the actin filament, with no nanosecond rotational motion (Thomas et al., 1979; Mossakowska et al., 1988; Ostap and Thomas, 1991) and is selectively bound to cys-374 (Thomas et al., 1979).

The large difference between the spectra of MSL-actin flowing perpendicular and parallel to the magnetic field (Fig. 2, *center* and *bottom*) clearly indicates a nonrandom angular distribution of spin labels relative to the flow axis. The spectrum of MSL-actin oriented parallel to the magnetic field was not accurately fitted by a single Gaussian orientational distribution (Fig. 4, Table 2), but the fit to a sum of Gaussian components was excellent (Fig. 5, Table 2).

There are three principal options for the assignment of the two components found in the fit of flowing MSL-actin. (*a*) Component A is the distribution of MSL-actin filaments oriented by flow, and component B is the dis-

tribution of MSL-actin filaments that remain disordered despite flow. (*b*) All of the actin is oriented by flow, and components A and B are the distributions of probes bound to different sites on actin. (*c*) All of the actin is oriented by flow, and component B is a state that is conformationally distinct from that reported in component A. Option (*b*) is unlikely because of previous studies showing that cys-374 is specifically labeled on F-actin by maleimide derivatives (Thomas et al., 1979; Sutoh, 1982; Lin et al., 1990). Thomas et al. (1979) showed that the labeling reaction saturated at one label per actin monomer. Even when the concentration of the added spin label was twice the actin concentration, the label-to-protein ratio was never significantly >1.0. In this study, the label-to-protein ratio is ~1:1, even though a 25% excess of free label was added during the labeling reaction, indicating the preferential labeling of one site. The MSL-S1 data provides evidence against options (*b*) and (*c*). It is not likely that S1 is disoriented relative to actin filaments in solution in the absence of ATP, since EM studies have consistently shown uniformly oriented rigor complexes (Moore et al., 1970). The spectrum of MSL-S1 bound to oriented actin is a linear combination of an ordered component, with approximately the same orientational distribution as MSL-S1 decorated fibers, and a disordered component. The mole fractions of these components are very similar to those of components A and B in MSL-actin (Table 2). If all of the actin filaments were ordered by flow, the spectrum of the MSL-S1 bound to actin would indicate a single orientational distribution, identical to the MSL-S1 decorated fibers (Table 2). Therefore, possibility (*a*) is the most likely assignment of the two components found in the computer fit.

Possible reasons for the incomplete ordering of a large fraction of the actin filaments (component B) include viscoelastic effects, actin aggregation, and adherence of the actin filaments to the capillary wall (Hard and Allen, 1985). A more complete study of MSL-actin orientation as a function of the velocity gradient and concentration is necessary to determine why all of the actin filaments do not completely order with flow (e.g., Harrington, 1981; Hard and Allen, 1985).

It was not possible to orient MSL-actin + S1 unless the S1 was dissociated from the actin filaments by ATP during the orientation process (Fig. 6). This observation strengthens the argument for S1-induced aggregation of actin filaments in solution (Ando and Scales, 1985; Ando, 1987; Ostap and Thomas, 1991). When oriented acto-S1 was produced, the computer fits indicated that the orientational distributions of MSL-actin ± S1 are not significantly different (Table 2). This implies that the axial orientation of actin protomers, as monitored by MSL at cys-374, is not significantly affected by the binding of S1 · MgADP. It is important to be confident that the ATP was depleted and the S1 had rebound to the oriented actin or the acquired spectrum would be equivalent to the MSL-actin spectrum. ATP depletion was confirmed by resuming the flow of the actin solution and observing greatly increased disorder.

The experiments with MSL-S1 not only helped with the identification of the distributions in the two component fit (see above), they also provided a measure of how well the actin is ordered compared with actin in the muscle fiber. The orientational distribution of the ordered component from the fit of the spectrum of MSL-S1 + actin oriented by flow was about the same as the orientational distribution of MSL-S1 bound to oriented fibers (Table 2). Thus, the oriented fraction of flow-oriented actin filaments has nearly the same high degree of alignment as the actin filaments in muscle fibers.

The errors reported in Table 1 and in Table 2 represent the standard deviations of the computer fits and probably underestimate the actual uncertainties. As can be seen in Table 2, the increase in standard deviation coincides with the increase in the number of protein preparations. Although it is theoretically possible to resolve angular differences of <1°, the variation in these samples do not justify such resolution. The relatively large standard deviations for both ϕ_0 and $\Delta\phi$ are expected because of the weak dependence of the spectrum on the orientation of the minor axis with respect to the magnetic field (see Fig. 4 of Fajer et al., 1990*a*).

Relationship to other work

ST-EPR studies have demonstrated that S1 restricts MSL-actin's microsecond rotational motions (Thomas et al., 1979; Mossakowska et al., 1988; Ostap and Thomas, 1991). However, this restriction of the microsecond rotational motion may be due in part to S1-induced aggregation of the actin filaments rather than a change in the conformation of actin protomers (Ando and Scales, 1985; Ando, 1987; Ostap and Thomas, 1991). This study uses the same spin label and labeling method as the ST-EPR studies, and no changes are detected in the orientational distribution of the MSL-actin upon the binding of S1. This result supports the model of the restriction of microsecond rotational motion by S1-induced aggregation.

Fluorescence measurements of *N*-(1-pyrenyl)iodoacetamide specifically attached to cys-374 of actin indicate that the binding of S1 causes a quenching of the pyrene fluorescence of this label (Kouyama and Mihashi, 1981). These investigators have proposed that this change is due to a large-scale conformational change in the protein. However, EPR studies have demonstrated that MSL bound to cys-374 detects a change in polarity of the spin label's environment on the binding of S1 (Thomas et al., 1979), but no change is observed in the orientational distribution (this study). Crystallographic and cryoelectron microscopy data suggest that cys-374 is probably adjacent to the myosin binding site (Kabsch et al., 1990; Milligan et al., 1990). Therefore, it is possible that the pyrene group is detecting localized changes in the environment at the binding interface of actin and S1, not a

global conformational change. Further investigation of actin's conformation at the myosin binding site is required for clarification.

A number of other investigations also report conformational changes in the actin filament. Fluorescent phalloidin was used to detect orientational changes in F-actin during active tension development in glycerinated muscle fibers (Prochniewicz-Nakayama et al., 1983), resonance energy transfer was used to detect a S1-induced intramolecular distance change in actin (Miki et al., 1987), and fluorescent ADP derivatives were used to detect heavy meromyosin induced orientational changes in F-actin (Yanagida and Oosawa, 1978). These conformational changes might be undetectable in the present studies because either (*a*) the site at which actin is labeled (cys-374) is not sensitive to the changes or (*b*) these changes may only occur during the active interaction of myosin, actin, and ATP (Prochniewicz-Nakayama and Yanagida, 1982; Ando, 1989; Prochniewicz and Yanagida, 1990). Alternatively, it is possible that the S1-induced changes in the above studies do not reflect conformational changes in actin but reflect local rotations of the probes or their immediate environments (Fajer et al., 1990*b*). To investigate these possibilities more thoroughly, (*a*) spin labels should be attached to other sites on actin (e.g., the myosin binding site) or (*b*) caged ATP studies (Ostap and Thomas, 1991; Fajer et al., 1990*c*) should be done on oriented actin samples.

In conclusion, the spectra of flowing MSL-actin is best described by two orientational distributions, a highly ordered component, and a disordered component. The ordered component is representative of the actin filaments ordered by flow, and the disordered component is representative of actin filaments that remain disordered despite the flow. The actin filaments ordered by flow are nearly as well oriented as actin filaments in muscle fibers. The axial orientation of actin protomers is not significantly affected by the binding of S1 · MgADP to actin.

We thank C. L. Berger for providing the MSL-S1, R. L. H. Bennett, F. L. Nisswandt, P. G. Fajer, M. Karkoub, and J. J. Matta for technical and computer assistance. We also thank E. H. Egelman and R. Cooke for helpful discussions.

This work was supported by grants to D. D. Thomas from the National Institutes of Health (NIH) (AR-32961), and the Minnesota Supercomputer Institute. E. M. Ostap was supported by a Molecular Biophysics training grant from NIH (GM-08277-03).

Received for publication 17 December 1991 and in final form 24 June 1992.

REFERENCES

Ando, T. 1987. Bundling of myosin subfragment-1-decorated actin filaments. *J. Mol. Biol.* 195:351–358.

Ando, T. 1989. Propagation of acto-S1 ATPase reaction. Coupled conformational change in actin along the filament. *J. Biochem.* 105:818–822.

Ando, T., and D. Scales. 1985. Skeletal muscle myosin subfragment-1 induces bundle formation by actin filaments. *J. Biol. Chem.* 260:2321–2327.

Barnett, V. A., and D. D. Thomas. 1989. Microsecond rotational motion of spin-labeled myosin heads during isometric muscle contraction. *Biophys. J.* 56:517–523.

Barnett, V. A., P. Fajer, C. F. Polnaszek, and D. D. Thomas. 1986. High-resolution detection of muscle crossbridge orientation by electron paramagnetic resonance. *Biophys. J.* 49:144–146.

Berger, C. L., E. C. Svensson, and D. D. Thomas. 1989. Photolysis of a photolabile precursor of ATP (caged ATP) induces microsecond rotational motion of myosin heads bound to actin. *Proc. Natl. Acad. Sci. USA.* 86:8753–8757.

Borejdo, H., and H. Ortega. 1989. Electrophoresis and orientation of F-actin in agarose gels. *Biophys. J.* 56:285–293.

Cooke, R., M. S. Crowder, and D. D. Thomas. 1982. Orientation of spin-labeled myosin heads in contracting muscle fibers. *Nature (Lond.).* 300:776–776.

Eads, T. M., D. D. Thomas, and R. H. Austin. 1984. Microsecond rotational motions of eosin-labeled myosin measured by time-resolved anisotropy of absorption and phosphorescence. *J. Mol. Biol.* 179:55–81.

Egelman, E. H., N. Francis, and D. J. DeRosier. 1982. F-actin is a helix with a random variable twist. *Nature (Lond.).* 298:131–135.

Faber, R. J., and G. K. Fraenkel. 1967. Dynamic frequency shifts and the effects of molecular motions in the electron spin resonance spectra of dinitrobenzene anion radicals. 47:2462–2467.

Fajer, P. G., E. A. Fajer, N. J. Brunsvold, and D. D. Thomas. 1988. Effects of AMPPNP on the orientation and rotational dynamics of spin-labeled muscle cross-bridges. *Biophys. J.* 53:513–524.

Fajer, P. G., R. L. H. Bennett, C. F. Polnaszek, E. A. Fajer, and D. D. Thomas. 1990*a*. General method for multiparameter fitting of high-resolution EPR spectra using a simplex algorithm. *J. Mag. Res.* 88:111–125.

Fajer, P. G., E. A. Fajer, J. J. Matta, and D. D. Thomas. 1990*b*. Effect of ADP on the orientation of spin-labeled myosin heads in muscle fibers: a high resolution study with deuterated spin labels. *Biochemistry.* 29:5865–5871.

Fajer, P. G., E. A. Fajer, and D. D. Thomas. 1990*c*. Myosin heads have a broad orientational distribution during isometric muscle contraction: time-resolved EPR studies using caged ATP. *Proc. Natl. Acad. Sci. USA.* 87:5538–5542.

Fajer, P. G., E. A. Fajer, M. S. Schoenberg, and D. D. Thomas. 1991. Orientational disorder and motion of weakly attached cross-bridges. *Biophys. J.* 60:642–649.

Hard, R., and R. D. Allen. 1985. Flow birefringence of microtubules and its relation to birefringence measurements in cells. *Cell Motil.* 5:31–51.

Harrington, R. E. 1981. Structural conformations of nucleosomes at low ionic strength from flow birefringence and intrinsic viscosity. *Biopolymers.* 20:719–752.

Houk, W., and K. Ue. 1974. The measurement of actin concentration in solution: a comparison of methods. *Anal. Biochem.* 62:66–74.

Huxley, A. F. 1974. Muscular contraction. *J. Physiol. (Lond.).* 243:1–43.

Huxley, A. F., and R. Simmons. 1971. Proposed mechanism of force generation in striated muscle. *Nature (Lond.).* 233:533–538.

Huxley, H. E. 1969. The mechanism of muscular contraction. *Science (Wash. DC).* 164:1356–1366.

Kabsch, W., H. G. Mannherz, D. Suck, E. F. Pai, and K. C. Holmes.

1990. The structure of the actin-DNase I complex. *Nature (Lond.).* 347:37–44.

Kouyama, T., and K. Mihasi. 1981. Fluorimetry study of N-(1-pyrenyl)iodoacetamide-labeled F-actin. *Eur. J. Biochem.* 114:33–38.

Lin, T. I., M. Kim, and R. M. Dowben. 1990. Accessibility of thiols in actin—a kinetic study with fluorescent maleimide probes. *Prog. Clin. Res.* 327;771–778.

Margossian, S. S., and S. Lowey. 1982. Preparation of myosin and its subfragments from rabbit skeletal muscle. *In* Methods in Enzymology. D. W. Frederiksen and L. W. Cunningham, editors. Academic Press, New York. 55–71.

Miki, M., and K. Mihashi. 1977. Fluorescence and flow dichroism of F-actin-ADP; the orientation of the adenine plane relative to the long axis of F-actin. *Biophys. Chem.* 6:101–106.

Miki, M., C. G. dos Remedios, and J. A. Barden. 1987. Spatial relationship between the nucleotide-binding site, Lys-61, and Cys-374 in actin and a conformational change induced by myosin subfragment-1 binding. *Eur. J. Biochem.* 168:339–345.

Milligan, R. A., M. Whittaker, and D. Safer. 1990. Molecular structure of F-actin and location of surface binding sites. *Nature (Lond.).* 348:217–221.

Moore, P. B., H. E. Huxley, and D. J. DeRosier. 1970. Three-dimensional reconstruction of F-actin, thin filaments, and decorated thin filaments. *J. Mol. Biol.* 50:279–295.

Mossakowska, M., J. Belagyi, and H. Strzelecka-Golaszewska. 1988. An EPR study of the rotational dynamics of actins from striated and smooth muscle and their complexes with heavy meromyosin. *Eur. J. Biochem.* 175:557–564.

Ostap, E. M., and D. D. Thomas. 1991. Rotational dynamics of spin-labeled F-actin during activation of myosin S1 ATPase using caged ATP. *Biophys. J.* 59:1235–1241.

Pardee, J. D., and J. A. Spudich. 1982. Purification of muscle actin. *In* Methods in Enzymology. D. W. Frederiksen and L. W. Cunningham, editors. Academic Press, New York. 164–181.

Popp, D., V. V. Lednev, and W. Jahn. 1987. Methods of preparing well-oriented sols of F-actin containing filaments suitable for X-ray diffraction. *J. Mol. Biol.* 197:679–684.

Prochniewicz, E., and T. Yanagida. 1990. Inhibition of sliding movement of F-actin by crosslinking emphasizes the role of actin structure in the mechanism of motility. *J. Mol. Biol.* 216:761–772.

Prochniewicz-Nakayama, E., and T. Yanagida. 1982. The effect of crosslinking of thin filament with glutaraldehyde on the contractility of muscle fiber. *J. Biochem.* 92:1269–1277.

Prochniewicz-Nakayama, E., T. Yanagida, and F. Oosawa. 1983. Studies on conformation of F-actin in muscle fibers in the relaxed state, rigor, and during contraction using fluorescent phalloidin. *J. Cell Biol.* 97:1663–1667.

Reedy, M. K., K. C. Holmes, and R. T. Tregear. 1965. Induced changes in orientation of the cross-bridges of glycerinated insect flight muscle. *Nature (Lond.).* 207:1276–1280.

Squier, T. C., and D. D. Thomas. 1986. Methodology for increased precision in saturation transfer electron paramagnetic resonance studies of rotational dynamics. *Biophys. J.* 49:921–935.

Sutoh, K. 1982. Identification of myosin-binding sites on the actin sequence. *Biochemistry.* 21:3654–3661.

Svensson, E. C., and D. D. Thomas. 1986. ATP induces microsecond rotational motions of myosin heads crosslinked to actin. *Biophys. J.* 50:999–1002.

Thomas, D. D. 1987. Spectroscopic probes of muscle cross-bridge rotation. *Annu. Rev. Physiol.* 49:891–909.

Thomas, D. D., and R. Cooke. 1980. Orientation of spin-labeled myosin heads in glycerinated muscle fibers. *Biophys. J.* 32:891–906.

Thomas, D. D., J. C. Seidel, and J. Gergely. 1979. Rotational dynamics of spin-labeled F-actin in the sub-millisecond time range. *J. Mol. Biol.* 132:257–273.

Torbet, J., and M. J. Dickens. 1984. Orientation of skeletal muscle actin in strong magnetic fields. *FEBS (Fed. Eur. Biochem. Soc.) Lett.* 173:403–406.

Yanagida, T., and F. Oosawa. 1978. Polarized fluorescence from ϵ-ADP incorporated into F-actin in a myosin-free single fiber: conformation of F-actin and changes induced in it by heavy meromyosin. *J. Mol. Biol.* 126:507–524.